ELSEVIER

Polymer 43 (2002) 4957–4965

polymer

www.elsevier.com/locate/polymer

The effect of short chain branching on local chain organisation in isotopically labelled blends of polyethylene

Sandry Coutry, Stephen J. Spells*

Materials Research Institute, Sheffield Hallam University, City Campus, Sheffield S1 1WB, UK

Received 31 January 2002; accepted 22 May 2002

Abstract

The complementary techniques of small angle neutron scattering (SANS) and infra-red spectroscopy have been used to determine features of molecular trajectory for isotopic blends incorporating linear polyethylene and copolymers containing butyl or hexyl branches. SANS data show both a more compact conformation for a copolymer guest molecule than for a linear guest and also a smaller molecular expansion with increasing molecular weight when both guest and host are copolymers. These blends also show the smallest proportion of {110} isolated guest stems, while wholly linear blends show the largest proportion, on the evidence of the infra-red CD_2 bending band profiles. Estimates are made of the sizes of 'groups' of adjacent stems, and these also show a corresponding dependence on the sample type, indicating a higher proportion of adjacent re-entry for copolymer blends than for linear blends.

Keywords: Molecular trajectory; Polyethylene; Adjacent re-entry

1. Introduction

In view of the commercial importance of the drawing of polymers such as polyethylene, it is necessary to understand the factors which control mechanical properties. Several key questions—such as the formation and behaviour during deformation of tie-chains—remain unanswered. Metallocene catalysed polymers are of increasing importance commercially and, having narrow molecular weight distributions and controllable, homogeneous branch contents, they are well adapted for use in fundamental studies of structure–property relationships. As part of a larger project with the objective of studying changes in molecular conformation in isotopic blends of homopolymers and copolymers during drawing, we initially characterised these blends after melt quenching and prior to deformation.

In combination, elastic neutron scattering and mixed crystal infra-red spectroscopy (MCIRS) provide detailed information on molecular conformation. Their combined use was developed in the study of PE single crystals, and the resulting statistical models fully describe the arrangement of crystal stems (the individual molecular traverses of the chain-folded crystals) [1]. Progress with melt crystallised PE has been slower, in part because of the tendency towards isotopic fractionation, even in blends of linear polymers. In common with much of the earlier work, we limit ourselves here to crystallisation rates which are sufficiently high as to minimise isotopic fractionation. This involves the quenching of molten blended polymers into cold water. The narrow molecular weight distributions obtainable from metallocene-polymerised materials are particularly important here in the interpretation of combined MCIRS and SANS data.

Intermediate angle neutron scattering (IANS) measurements have provided the main evidence for the chain conformation in quenched linear PE. While small angle data indicate little change in radius of gyration on crystallising from the molten state [2], the IANS is sensitive to the local stem arrangement: data have been fitted using the 'solidification' model, with the minimum movement of chain segments during crystallisation [3] and the 'subunit' model, where a large local rearrangement of the chain allows folding to occur, but the distribution of subunits is determined by the Gaussian chain conformation in the melt [4]. The latter model involves short rows of adjacent stems, without preference for any crystallographic fold direction. It was estimated that up to 40% of chain folds may be adjacent, a drastically smaller proportion than in single crystals [1].

The MCIRS technique has previously been applied to isotopic blends of linear PE crystallised by cooling at

* Corresponding author. Tel.: +44-114-225-3428; fax: +44-114-225-3066.

E-mail address: s.j.spells@shu.ac.uk (S.J. Spells).

0032-3861/01/$ - see front matter
PII: S0032-3861(02)00334-8

around 1 °C min^{-1} from the melt [5]. The CD_2 bending vibration was used to monitor the arrangement of chain stems for the 'guest' species. As the bandwidth at liquid nitrogen temperatures was found to be greater than for 'model' *n*-alkane mixtures, it was inferred that a doublet component was present. Curve fitting resulted in an estimate of 30–40% of crystal stems being in adjacent arrangements, with the CD_2 bending doublet splitting reaching a value of about 3.1 cm^{-1} for the highest molecular weights studied. This corresponds to a group of approximately three adjacent {110} stems. Low temperature MCIRS data for a melt quenched PE blend show clearer evidence of a CD_2 bending doublet, in addition to the singlet arising from disordered chains and deuterated crystal stems which are isolated from others in ⟨110⟩ directions [6]. Spectral deconvolution showed the doublet splitting to be 3.4 cm^{-1}, indicating a similar group size.

As with blends of linear PE, mixtures of linear and branched PE have also been studied in relation to their miscibility. A series of papers by Hill et al., involving the rapid quenching of PE blends, have combined DSC experiments with transmission electron microscopy (TEM) of surface replicas. The regions of double morphology arising from liquid–liquid phase separation (LLPS) in the molten state have been mapped, and these studies have included metallocene-catalysed copolymers [7,8]. In general, a closed loop biphasic region is obtained at less than around 50% of linear PE in the case of linear/branched blends, and a similar loop is observed in blends of low density PE. In this case, the branch content was found to be the key quantity: two components with similar branch contents tend to result in a single morphology, while the type of branch or the method of polymerisation used (metallocene-catalysed or other) were found to have less significance. This conclusion has, in view of recent micro-Raman imaging work, been revised to link the biphasic morphology with different degrees of crystallinity for linear and branched components [9]. It should be noted, though, that all these measurements on blends refer to LLPS, rather than fractionation of species during crystallisation.

On the other hand, the use of SANS to monitor phase separation has led to disagreement with the interpretations from TEM work [10]. Excess SANS intensity has long been used to detect and quantify isotopic fractionation and, by evaluating SANS data from similar linear/branched PE blends, 'it should be clear that SANS can easily detect concentration fluctuations accompanying LLPS that are difficult to observe by other methods' [10]. In a study of model polyolefins, Balsara and co-workers [11] showed that both SANS (through enhanced forward scattering) and light scattering (through the presence of a spinodal ring) were in agreement in identifying two-phase structures. For a range of molten linear/branched PE blends, Alamo et al. [12] showed that the mixtures were homogeneous for low branch contents (<4 branches/100 backbone C atoms) and that phase separation occurred at branch contents ≥ 8 branches/100 backbone C atoms. Results based on TEM microstructures should, therefore, be viewed with some caution as a guide to the morphologies expected for the blends studied here.

MCIRS works on blends of linear and branched PE has been limited. Sasaki et al. [13] chose to use blends of high density deuterated PE (DPE) with branched hydrogenous PE in order to avoid isotopic fractionation on crystallisation by slow cooling from the melt. However, measurements at room temperature do not allow a full analysis of the crystal stem distributions.

A reduction in the crystallinity of PE with increasing branch content is well known, but it has recently been shown that, for both low density and linear low density PE, the crystallinity as determined by Raman spectroscopy is significantly less than that measured by DSC or wide angle X-ray scattering (WAXS) [14]. Since the Raman technique is associated with the orthorhombic crystal structure, it was proposed that a proportion of disrupted orthorhombic material is detected by the other methods, but not by Raman spectroscopy. In addition, recent WAXS measurements on PE materials with a range of branch contents indicate that the orthorhombic unit cell *a* and *b* dimensions both increase with increasing branch content [15]. This may be related to some incorporation of branches into the crystallites. In terms of the MCIRS results considered here, the increase in *a* and *b* dimensions will lead to a decrease in the maximum doublet splittings obtainable for the branched components of blends.

Metallocene-catalysed PE and copolymers are particularly useful in providing relatively uniform materials for studying changes in molecular conformation with deformation. As a precursor to these studies, it was necessary to characterise the melt-quenched starting samples for different linear and copolymer combinations as guest and matrix in isotopic blends.

2. Experimental details

2.1. Sample preparation

A range of linear and metallocene-catalysed copolymer PE samples were used. Linear hydrogenous samples A and B and linear deuterated samples 1–3 were kindly supplied by Dr P.J. Barham, University of Bristol. These were prepared from commercial materials by liquid–liquid fractionation. All the other samples were produced by BP Chemicals and kindly provided by Dr W. Reed. GPC characterisation was obtained from the University of Bristol and BP Chemicals, and the extent of side chain branching in copolymer samples was determined by BP Chemicals. The materials used are specified in Table 1.

In order to blend isotopic species in small quantities, solution mixing was used. Hydrogenous and deuterated (3 or 5%, w/w) polymers were mixed at 1% total w/w in xylene

Table 1
Characterisation of polyethylene materials used

Material identifier	Type[a]	$\bar{M}_w \times 10^{-3}$	$\bar{M}_n \times 10^{-3}$	$\bar{M}_w/\bar{M}_n$	Side chain branches[b]
1	LD	76	55	1.4	–
2	LD	95	48	2.0	–
3	LD	136	77	1.8	–
4	LDM	413	157	2.6	–
5	CDM	95	11	8.6	6.3 C_6
6	CDM	378	181	2.1	8.0 C_4
A	LH	86	24	3.6	–
B	LH	90	30	3.0	–
C	LH	134	18	7.6	–
D	LH	385	48	8.0	–
E	CH	181	15	12.1	6.0 C_4

[a] L denotes a linear polymer; C a copolymer; D a deuterated polymer; H a hydrogenous polymer and M a material polymerised by a metallocene catalysis process.
[b] Number of short chain branches per thousand backbone carbon atoms.

and heated to boiling. Mixing was continued for 30 min, after which the solution was added to excess methanol to precipitate the samples. The mixture was then filtered and dried, with a final stage under vacuum at 70 °C for 8 h. Aluminium packages of these blends were heated to 160 °C in a press for 15 min before removal and quenching into cold water. In this way, films of approximately 0.3 mm thickness were made. Solution blending may result in a change in the sample deuterium concentration, since the precipitation may be incomplete. An FTIR technique was adopted to determine the final concentration of the deuterium species, using the ratio of the integrated areas of CH_2 and CD_2 bending vibrations. Deviations from the initial deuterium concentrations were generally small, with a maximum discrepancy of 2.3% (starting and final concentrations of 5.0 and 7.3%).

WAXS was undertaken to determine whether the samples had any initial crystallite orientation or any monoclinic material. A Worhus flat plate camera and a MarResearch image plate detector (the latter courtesy of Dr G. Ungar, University of Sheffield) were both used with filtered copper K_α radiation for thin sample films perpendicular and parallel to the beam. No signs of preferred orientation were seen, and neither was there any indication of crystallographic peaks from the monoclinic crystal form.

The nomenclature used to identify samples can be explained with reference to sample CL/95/385. In this example, the deuterated guest molecule is a copolymer (C) with molecular weight, $\bar{M}_w$, of 95 000 (95), while the hydrogenous host is a linear polymer (L), with $\bar{M}_w$ of 385 000 (385). The individual polymer characteristics can then be identified by reference to Table 1. For this example, the polymers can be identified as 5 and D.

The absence of isotopic fractionation in isotopic blends such as these is important in the interpretation of SANS and MCIRS data. It has been widely noted that the SANS technique allows an assessment of the extent of fractionation [13]. Similarly, the splitting of the infra-red CD_2 bending vibration can reveal gross effects [16], as this approaches the value for the pure deuterated polymer. A sample of LL/76/86 was prepared by cooling a melt at around 0.5 °C min^{-1}. On cooling the sample to liquid nitrogen temperatures, a maximum splitting of 9.8 cm^{-1} was obtained, compared with 10.2 cm^{-1} for the pure deuterated polymer, thus indicating gross isotopic fractionation.

2.2. Neutron scattering

SANS measurements were made using the instruments LOQ (CCLRC, Didcot, England) and D11 (ILL, Grenoble, France). The range of scattering wavevector, q ($q = 4\pi \sin\theta/\lambda$), where 2θ is the scattering angle and λ the neutron wavelength), for LOQ was from 8×10^{-3} to 0.25 $Å^{-1}$. Samples were in the form of stacks of 10×10 mm^2, wrapped in aluminium foil and held in cadmium holders with an aperture of 8 mm diameter defining the beam size. Data reduction (including azimuthal averaging) and analysis were mostly undertaken using the Collette program at ISIS, with the usual corrections for sample cell and the use of a hydrogenous sample to determine the incoherent scattering. Measurements on D11 involved a helical slot velocity selector, providing a resolution of 10% with a wavelength distribution peaked at 8.5 Å. The accessible q range was from 0.005 to 0.02 $Å^{-1}$. Similar sampling and data reduction and analysis were used.

2.3. FTIR

A Mattson Galaxy 6021 spectrometer was used, with an MCT detector. The sample was mounted in a Graseby-Specac 21500 cryostat, used in conjunction with a 20120 temperature controller. The sample space was evacuated. A dry air purge minimised interference from water and carbon dioxide vapour. A spectral resolution of 1 cm^{-1} was employed, with typically around 100 scans. Mattson

Table 2
Radius of gyration (R_g) and molecular weight ($\bar{M}_w$) for the different combinations of deuterated (DPE) guest in hydrogenated (HPE) host measured using the LOQ instrument at ISIS (Didcot, England) and the D11 instrument at ILL (Grenoble, France)

Sample identifier	LOQ		D11	
	R_g (Å)	$\bar{M}_w$ ($\times 10^{-3}$)	R_g (Å)	$\bar{M}_w$ ($\times 10^{-3}$)
LL/136/86	233 ± 42	160 ± 19	–	–
LL/95/86	236 ± 31	150 ± 13	–	–
LL/76/86	155 ± 15	63 ± 2	–	–
LL413/90	260 ± 18	413*	–	–
LL/95/385	269 ± 14	95*	291 ± 15	95*
LL/413/385	509 ± 40	413*	543 ± 45	413*
LL/413/385/MM	408 ± 33	413*	376 ± 43	413*
LC/95/181	319 ± 34	175 ± 25	318 ± 21	102 ± 4
LC/413/181	–	–	618 ± 33	413*
CL/378/385	363 ± 41	570 ± 42	371 ± 35	310 ± 20
CL/95/385	209 ± 14	144 ± 6	–	–
CC/95/181	–	–	237 ± 18	146 ± 7
CC/378/181	–	–	410 ± 27	308 ± 14

* indicates samples where the intercept was fixed during the process of the linear fitting of the SANS data, using the molecular weight as measured by GPC. MM indicates a sample blended by mixing in the melt state.

software was used for the Fourier self-deconvolution of spectra.

3. Results

3.1. Neutron scattering

Samples primarily made use of matrix polymers A, D and E in Table 1. For the deuterated linear (2) and copolymer (5) with $\bar{M}_w = 95\,000$, Zimm plots were generally highly linear, with the exception of sample LL/95/385. The small excess scattering in this latter case still allowed extrapolation to the forward scattering expected for the molecular weight. For guest polymer 4, some curvature was noted in Zimm plots, using either of polymers D or E as matrix. This resulted in fitting over only a small number of data points. In these cases, the $I(0)$ intercepts were fixed to correspond with the known values of $\bar{M}_w$. Some catalyst residue was detected in sample 4, using X-ray fluorescence measurements, and this may be responsible for introducing another source of contrast. Collected SANS results for a range of samples are shown in Table 2.

Some general comments can be made in relation to this data. First, data from LOQ and D11 are in good agreement. A weighted average of LOQ and D11 results was therefore used where possible, for further analysis. Second, when considering the $\bar{M}_w$ values obtained from the Zimm plots (setting to one side those cases where the intercept $I(0)$ was fixed), there is little indication of isotopic fractionation: indeed, the values obtained by GPC usually agree with these to well within a factor of 2, which is generally taken as evidence of good miscibility [17]. For LL samples, the values of radius of gyration (R_g) are similar to those listed by Sadler and Barham [18]. These values are all somewhat higher than previously published data for melt-quenched PE films [19–22]. A possible explanation is that, as in Ref. [18], an unfractionated matrix was used here.

Table 3
The exponent α for different types of sample, obtained as a function of the molecular weight of the DPE guest ($R_g \propto \bar{M}_w^{\alpha}$)

Sample identifier	α
LL/X/385	0.48 ± 0.04
CL/X/385	0.45 ± 0.06
LC/X/181	0.48 ± 0.03
CC/X/181	0.40 ± 0.05

From the data in Table 2, plots of log R_g versus log $\bar{M}_w$ yield the exponent α in the expression

$$R_g \propto \bar{M}_w^{\alpha}$$

Carrying out this procedure separately for the different guest/host combinations yielded the results shown in Table 3. All figures are slightly lower than the 0.5 predicted for a random coil. The CC value of 0.40, although agreeing with the other values to within the quoted errors, may point to a difference in molecular conformation: the result suggests that the molecular expansion with increasing molecular weight is rather more limited than for the other three systems listed. Two of the factors affecting R_g will now be considered.

3.1.1. The replacement of linear guest DPE with its copolymer counterpart

Table 4 shows relevant data for low and high molecular weight guest species. In general, a decrease of around 20–30% accompanies this change, where the molecular weights of guest and matrix are kept similar. Estimates are given in the tables for the 'linear equivalent' R_g for the copolymer guest molecules, based on the 'backbone molecular weight' of the copolymer (i.e. neglecting branches) and using the appropriate exponent α quoted in Table 3. It is notable that

Table 4
Average values of R_g for samples containing (a) low and (b) high molecular weight DPE

Sample identifier	$\langle R_g \rangle$ (Å)	R_{gL} (Å)
(a) Low molecular weight DPE		
LL/95/385	279 ± 10	
CL/95/385	209 ± 14	251 ($\bar{M}_{wL} = 91\,000$)
LC/95/181	318 ± 12	
CC/95/181	237 ± 18	262 ($\bar{M}_{wL} = 91\,000$)
(b) High molecular weight DPE		
LL/413/385	524 ± 30	
CL/378/385	367 ± 26	484 ($\bar{M}_{wL} = 367\,000$)
LC/413/181	618 ± 33	
CC/378/181	410 ± 27	513 ($\bar{M}_{wL} = 367\,000$)

R_{gL} is the radius of gyration of a linear DPE of equivalent $\bar{M}_w$ to the copolymer guest backbone.

Table 5
Curve fitting results on the deconvoluted data for the low molecular weight guest samples

Sample identifier	χ_c (%)	Outer splitting (cm^{-1})	Singlet area (%)	Doublet area (%)	S_c (%)	d_c (%)
LL/95/385	53	5.6	60	40	44	56
CL/95/385	52	6.5	58	42	42	58
CC/95/181	38	8.5	62	38	38	62

The DSC crystallinities of the samples are listed in column χ_c; the separation of the outermost peaks are listed in the column 'Outer splitting'; the normalised areas of the singlet and doublet components are shown, followed by the normalised areas of the singlet (s_c) and doublet (d_c) components without the contribution from amorphous regions.

copolymer guest R_g values are still systematically smaller than for the linear guest blends. A more compact molecular conformation is thus indicated for the copolymer guest blends.

3.1.2. The replacement of linear matrix PE with its copolymer counterpart

Referring again to Table 4, it can be seen that this replacement leads to an increase in R_g of around 10–20%. These differences are similar to the uncertainties in R_g, but the direction of change is consistent. In a copolymer matrix, the guest molecule seems to have a slightly larger R_g than in a linear matrix. Preferential exclusion of side chains from crystals and the resulting decrease in crystallinity, as compared with linear polymers, may be a key factor here. However, the fact that the direction of change is the reverse of that seen in the previous section for substitution of guest species suggests some caution in the interpretation.

To explore the local molecular arrangement in further detail, it is necessary to use MCIRS.

3.2. MCIRS

MCIRS, using the profile of the CD_2 bending vibration at liquid nitrogen temperatures, provides information on the proportion of labelled crystal stems which are isolated from other labelled stems in ⟨110⟩ directions, using the absorbance of the central singlet. In addition, the various doublet components relate to groups of stems with ⟨110⟩ nearest neighbours, their splittings increasing with the size of group.

Initially, spectra were normalised, using the integrated absorbance over the entire CD_2 bending region. Fourier self-deconvolution was then used to improve the spectral resolution, in order to distinguish some of the spectral components. Typical values for the deconvolution parameters were 2.5 cm^{-1} for the full width at half maximum of the intrinsic lineshape and an enhancement factor of 3.0. Two methods of analysis were then employed. The first of these was a simple curve fitting procedure, using a singlet plus the minimum number of doublet components necessary to achieve a good fit. This normally involved up to five Voigt functions (combining the characteristics of Lorentzian and Gaussian functions). However, the frequencies so obtained should not be interpreted as corresponding to the only groups present in the structures. It is particularly clear for single crystal PE samples that spectra include contributions from many doublets, with separations which can be very small [23]. The fits should therefore be seen as representing 'average' group sizes present. This shortcoming of the technique led to the second method of analysis, which involved using the splittings previously calculated for the smallest group sizes (two ⟨110⟩ adjacent stems, three ⟨110⟩ adjacent stems, etc.). The frequencies of the high and low frequency components could then be calculated. It was found necessary to slightly modify the equations given in Ref. [24] to give

$$\nu_{high} = 1087.4 + 0.56\Delta\nu\ cm^{-1},$$
$$\nu_{low} = 1087.4 - 0.44\Delta\nu\ cm^{-1} \quad (1)$$

where ν_{high} and ν_{low} are the frequencies of the two components with a splitting of $\Delta\nu$. The reason for this modification is not clear, although it may relate to a slight variation in the unit cell dimensions. Having obtained a list of frequencies for the various smaller groups, these were then combined to match the deconvoluted experimental data as close as possible. While this procedure does not strictly constitute a 'fit', it has some advantages over the first method, in making use of known information about possible frequency components.

MCIRS data for three samples involving low molecular weight guest molecules are shown in Fig. 1. The raw data appear similar, although some differences become apparent after deconvolution. The results of curve fitting the deconvoluted data are shown in Table 5. As has been explained elsewhere [24], curve fitting the deconvoluted rather than the raw data provides a more constrained fit, while the deconvolution process conserves peak areas. In each case, fits involved the central singlet and three or four doublet pairs. Table 5 also includes values of crystallinity obtained from DSC measurements. This enables the singlet area to be decomposed into contributions from both amorphous chains and isolated labelled crystal stems. The maximum splitting of 5.6 cm^{-1} for sample LL/95/385 corresponds [23] to groups of four adjacent labelled stems distributed in two adjacent (110) planes. In the terminology developed elsewhere [25], this is denoted a 2×2 group. By contrast, the outermost splitting of 6.5 cm^{-1} for sample CL/95/385 corresponds to groups of 2×3 to 4×2 adjacent

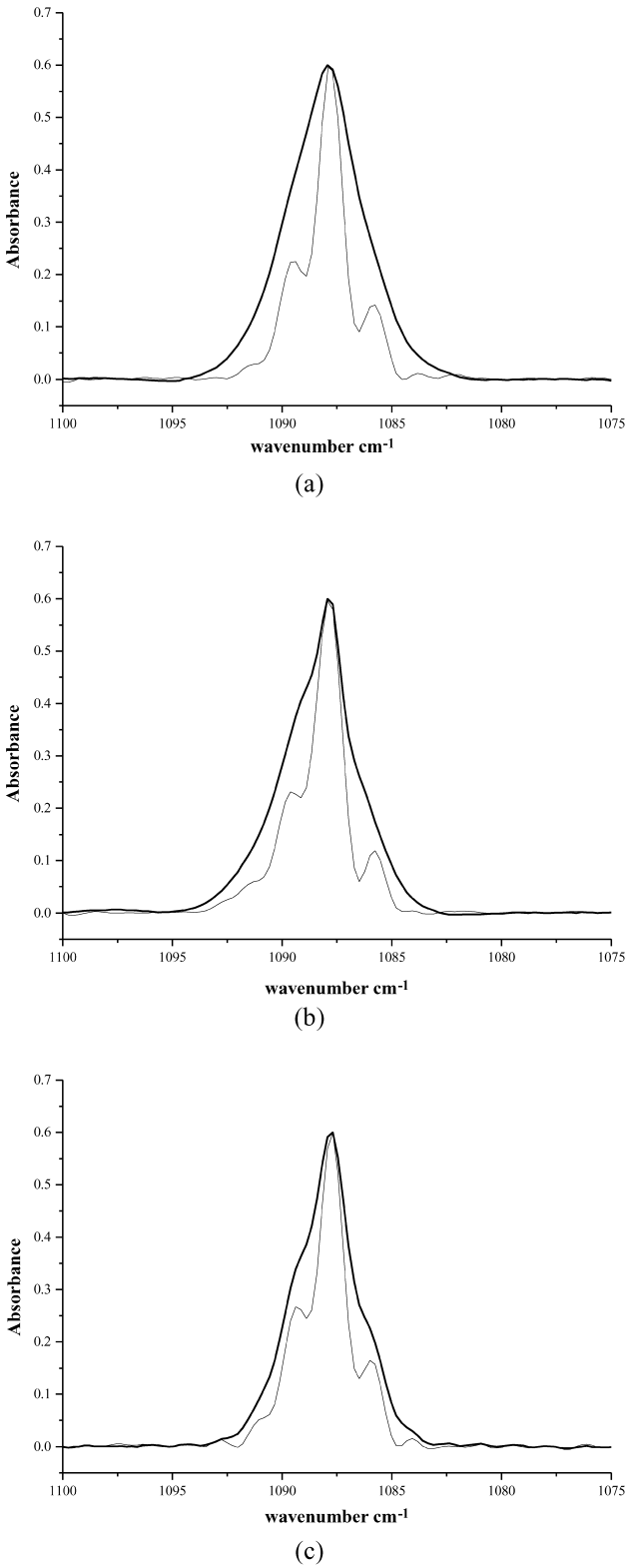

Fig. 1. The CD_2 bending region of the samples: (a) LL/95/385; (b) CL/95/385; (c) CC/95/181. The thick lines represent the raw data, while the fine line shows deconvoluted data. All the measurements were made at −170 °C.

labelled stems and the splitting of 8.5 cm^{-1} for sample CC/95/181 to groups of 3 × 4 adjacent labelled stems. While the largest group sizes are clearly quite different, ranging from 4 to 12 labelled stems, it should be remembered that these groups only represent a very small proportion of the sample. After the removal of the contribution from amorphous chains, the percentages of stems which are isolated, and hence contribute to the singlet, shows more variation: 56% of crystal stems in LL/95/385 are in groups of more than one, while this figure rises to 62% for CC/95/181. The implication is that the copolymer guest molecule gives rise to more adjacent folding than the linear guest, and that this effect is enhanced by the presence of copolymer matrix.

Fig. 2 and Table 6 show MCIRS results for higher molecular weight guest molecules. The CD_2 bending profiles are generally broader than those in Fig. 1. Sample LL/413/385 shows a very similar proportion of crystal stems which are isolated from ⟨110⟩ neighbours to sample LL/95/385, although the outermost splitting is larger (7.8 cm^{-1}, 3 × 3 group). Most of the stems, however, are still in groups of four or less. The 'subunit' model for melt-crystallised PE [4], with its small groups of adjacent stems, would lead to little change in the CD_2 bending profile with increasing molecular weight. This is in contrast to the strong dependence on molecular weight for solution-crystallised PE [1], due to the propensity for adjacent folding. Samples CL/378/385 and CC/378/181 both show a marked decrease in the proportion of isolated crystal stems, by comparison with their lower molecular weight analogues (Table 5). Again, the distribution in terms of group sizes is similar to the low molecular weight case. While the outermost splitting for CC/378/181 is the same as for CC/95/181, the proportion of stems contributing to this splitting is greater for the high molecular weight sample.

From both sets of data (Figs. 1 and 2, Tables 5 and 6), copolymer guest molecules appear to slightly favour the formation of groups of adjacent stems. However, in all cases the majority of stems are in very small groups. The effect of branches in constraining the geometry of the crystal fold may be significant here.

In order to compare experimental data with known doublet splittings, these splittings were firstly calculated for the smallest possible groups (e.g. 2 × 1, 3 × 1, 4 × 1, 2 × 2, 3 × 2, etc.). A total of 34 doublets were considered, each component being represented by a Lorentzian. Eq. (1) was used to calculate the component peak frequencies, given $\Delta\nu$. Contributions from these components were then summed together on a trial-and-error basis, to obtain the best possible correspondence with deconvoluted data. Typical results are shown in Fig. 3. While the match is not ideal, the main features of the spectra are clearly reproduced. At large splittings, some discontinuities are apparent in the calculated curves. These correspond to the cut-offs used with the Lorentzian profiles. To account for the difference in absorbance between the high and low frequency doublet components, a scaling factor was introduced for the low

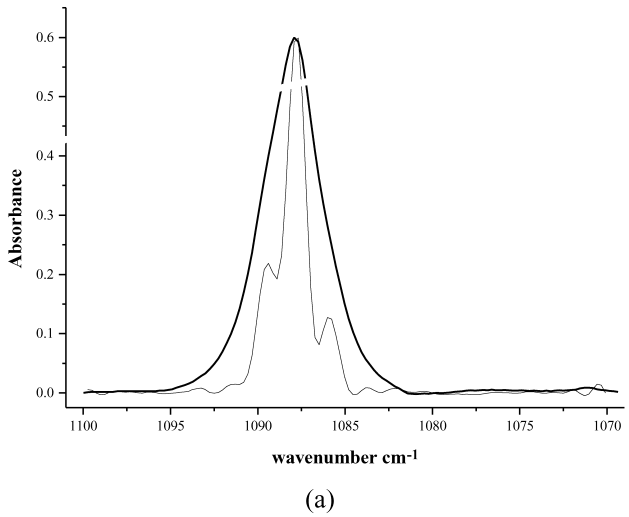

Fig. 2. The CD_2 bending region of samples: (a) LL/413/385; (b) CL/378/385; (c) CC/378/181. The thick lines represent the raw data, while the thin line shows the deconvoluted data. All measurements were made at −170 °C.

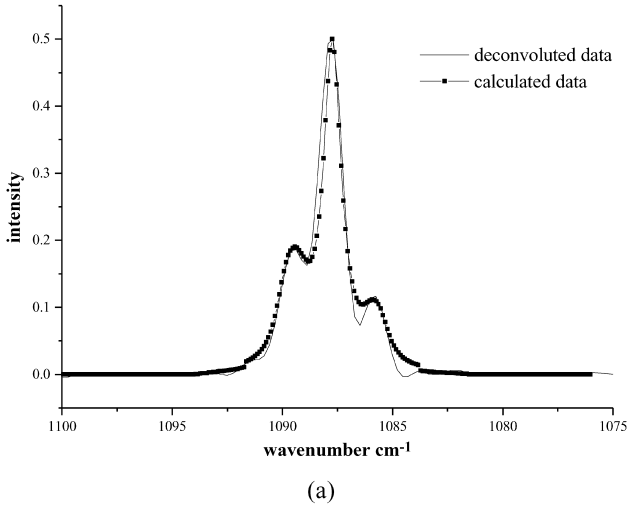

Fig. 3. CD_2 bending profile for samples: (a) LL/95/385; (b) CL/95/385; and (c) CC/95/181. A continuous line shows deconvoluted experimental data, the line with squares shows calculated data.

Table 6
Curve fitting results on the deconvoluted data for the low molecular weight guest samples

Sample identifier	χ_c (%)	Outer splitting (cm^{-1})	Singlet area (%)	Doublet area (%)	s_c (%)	d_c (%)
LL/413/385	49	7.8	62	38	45	55
CL/378/385	50	8.5	53	47	36	64
CC/378/181	38	8.5	54	46	21	79

The DSC crystallinities of the samples are listed in column χ_c; the separation of the outermost peaks are listed in the column 'Outer splitting'; the normalised areas of the singlet and doublet components are shown, followed by the normalised areas of the singlet (s_c) and doublet (d_c) components without the contribution from amorphous regions.

frequency component. As with the curve fitting, the contribution to the singlet from amorphous chains was removed. To analyse the results, groups were divided, quite arbitrarily, into three different categories; small (2×1 to 4×1 groups), medium (5–7 stems in 1 or 2 planes) and large (8–12 stems in 2 or 3 planes).

Table 7 shows results for three samples containing low molecular weight guest species. The proportions of labelled crystal stems which are isolated from similar nearest neighbours are similar to those shown in Table 5, but it is now clear that the fraction of stems in 'medium' or 'large' groups increases on changing to a copolymer guest molecule. The results for sample LL/95/385 are similar to earlier measurements on melt quenched PE [5], where it was suggested that 30–40% of stems were in adjacent configurations. Nevertheless, the results here suggest a rather higher level of adjacent folding, increasing still further for copolymer guest species.

Data for higher molecular weight guest molecules are shown in Table 8. Again, the results closely resemble those from curve fitting (Table 6). In addition, all three samples show significant, although still small, proportions of 'large' groups. The analysis confirms that, as in the case of lower molecular weight samples, copolymer guest samples tend to have a larger proportion of stems in groups.

4. Discussion

For the samples considered here, LLPS might be expected, on the basis of TEM surface replica studies [7], for blends of linear and branched polymers at less than 50% linear species. This condition applies to the LC type samples here. However, on the evidence of Alamo et al. [12], the branch content of both guest and matrix species used here is too low to produce a biphasic melt. Our SANS data show very little sign of isotopic fractionation in any sample, despite deviations from linearity in certain Zimm plots (sample 4). This appears to substantiate the conclusions of Alamo.

At this stage, we do not propose any specific statistical model for chain conformation in the blends studied. Such a model has been derived for PE single crystal samples [1], on the basis of IANS and MCIRS data. Here, we simply present some aspects of chain conformation, both on the scale of crystal stems and on the overall molecular scale. In future, IANS data may be used to construct a more detailed model, incorporating the probabilities of folding in different crystallographic directions.

From SANS measurements, the exponent α is close to 0.5 for all systems, apart from CC blends, which show a value of 0.40. This indicates a slower molecular expansion with increasing molecular weight for CC blends. Otherwise, the chain dimensions would be consistent with a random placement of crystal stems in the lattice although, as will be shown below, MCIRS data do not support this view. Changing from a linear to a copolymer guest molecule was shown to decrease its radius of gyration significantly, while changing from a linear to a copolymer matrix had a small, opposing effect, which may well lie within the experimental errors.

MCIRS data provide evidence of the extent of labelled stem adjacency, as well as the sizes of labelled stem groups. The proportion of labelled crystal stems which are isolated from labelled neighbours was shown to fall from 44% for LL/95/385 to 38% for CC/95/181, while for higher molecular weight guest molecules, the fall was from 45% for LL/413/385 to 21% for CC/378/181. The corresponding proportions of stems included in groups of at least two can be used as an upper estimate for the proportion of adjacent

Table 7
Stem distributions used to calculate the CD_2 bending profile for the low molecular weight guest samples

	LL/95/385 ($\chi_c = 53\%$)	CL/95/385 ($\chi_c = 52\%$)	CC/95/181 ($\chi_c = 38\%$)
Isolated stems (%)	50	42	38
Small groups (%)	46	42	58
Medium groups (%)	4	12	6
Large groups (%)	0	4	4
Max. splitting (cm^{-1})	4.2	8.1	8.1

χ_c is the crystallinity measured by DSC. The maximum splitting used in the calculation of the CD_2 bending profile is also listed.

Table 8
Stem distributions used to calculate the CD_2 bending profile for the high molecular weight guest samples

	LL/413/385 ($\chi_c = 49\%$)	CL/378/385 ($\chi_c = 50\%$)	CC/378/181 ($\chi_c = 38\%$)
Isolated stems (%)	50	34	29
Small groups (%)	43	56	63
Medium groups (%)	4	6	4
Large groups (%)	3	4	4
Max. splitting (cm^{-1})	7.2	8.5	8.5

χ_c is the crystallinity measured by DSC. The maximum splitting used to calculate the CD_2 bending profile of these samples is also listed.

folding. Adjacency of stems does not necessarily indicate adjacent re-entry, since near-to-adjacent folding and 'buried folds' may also be involved. The method is also insensitive to stem adjacency in directions other than ⟨110⟩. Nevertheless, it gives unique information about the local stem arrangement.

For LL combinations of guest and matrix, estimates for the proportion of adjacent stems (50–56%, according to Tables 5–8) are significantly higher than previous estimates of around 40% [4,5]. However, the best estimate here is probably nearer to the lower limit of the quoted range, since the method of analysis based on known group splittings (Tables 7 and 8) is probably more reliable. The proportion of adjacency within the crystals increases to 58–66% for a copolymer guest and to 62–71% for copolymer guest and matrix (Tables 7 and 8). The figures quoted here relate to the proportion of stems in groups of more than one {110} adjacent labelled stem. They are therefore rather greater than the probability of adjacent folding, since the groups are generally small.

For low molecular weight guest, the maximum group size detected increases from 4 stems for LL/95/385 to 6 or 8 stems for CL/95/385 and 12 stems for CC/95/181. Similarly, for higher molecular weights, the maximum size ranges from 9 stems for LL/413/385 to 12 stems for both CL and CC samples. It should, however, be noted that the majority of labelled stems are in much smaller groups. Nevertheless, the effect on group size of increasing molecular weight can be seen to be relatively minor, as predicted by the 'subunit' model.

This investigation has revealed small but significant differences in the guest molecular conformation in isotopic blends of PE homopolymer and copolymer. A copolymer guest molecule tends to have a more compact overall conformation than its linear counterpart, leading to larger groups, or subunits, of labelled stems. In addition, the increase in overall guest molecular dimensions with increasing molecular weight is smaller for copolymer samples than for linear blends. While this work does not provide a detailed statistical model for the structures, it does establish sufficient detail for understanding molecular rearrangements on cold drawing. This subject will be addressed in future papers.

Acknowledgments

We wish to thank BP Chemicals for supporting SC. We are indebted to Dr Warren Reed (BP Chemicals) and Dr Mary Vickers (University of Cambridge) for valuable discussions. We would also like to thank Dr Steve King (ISIS) and Dr Bruno Deme (ILL) for assistance with neutron scattering experiments.

References

[1] Sonntag P, Care CM, Spells SJ, Halliday I. J Chem Soc Faraday Trans 1995;91:2593.
[2] Schelten J, Wignall GD, Ballard DGH. Polymer 1974;15:682.
[3] Stamm M, Fischer EW, Dettenmaier M, Convert P. Discuss Faraday Soc 1979;68:263.
[4] Sadler DM, Harris R. J Polym Sci, Polym Phys Ed 1982;20:561.
[5] Jing X, Krimm S. J Polym Sci, Polym Lett Ed 1983;21:123.
[6] Spells SJ. Polym Commun 1984;25:162.
[7] Hill MJ, Barham PJ. Polymer 1997;38:5595.
[8] Hill MJ, Barham PJ. Polym Commun 2000;41:1621.
[9] Morgan RL, Hill MJ, Barham PJ, van der Pol A, Kip BJ, Ottjes R, van Ruiten J. Polymer 2001;42:2121.
[10] Crist B. Polymer 1997;38:3145.
[11] Balsara NP, Fetters LJ, Hadjichristidis N, Lohse DJ, Han CC, Graessley WW, Krishnamoorti R. Macromolecules 1992;25:6137.
[12] Alamo RG, Graessley WW, Krishnamoorti R, Lohse DJ, Londono JD, Mandelkern L, Stehling FC, Wignall GD. Macromolecules 1997;30:561.
[13] Sasaki S, Tashiro K, Gose N, Imanishi K, Izuchi M, Kobayashi M, Imai M, Ohashi M, Yamaguchi Y, Ohuyama K. Polym J 1999;31:677.
[14] Lagaron JM, Lopez-Quintana S, Rodriguez-Cabello JC, Merino JC, Pastor JM. Polymer 2000;41:2999.
[15] Baker AME, Windle AH. Polymer 2001;42:651.
[16] Spells SJ, Sadler DM, Keller A. Polymer 1980;21:1121.
[17] Sadler D, Barham PJ. Polymer 1990;31:38.
[18] Sadler DM, Barham PJ. J Polym Sci, Polym Phys Ed 1983;21:309.
[19] Summerfield GG, King JS. J Appl Cryst 1975;11:548.
[20] Schelten J, Ballard DGH, Wignall GD, Longman G, Schmatz W. Polymer 1976;17:751.
[21] Sadler DM, Keller A. Science 1979;203:263.
[22] Ballard DGH, Burgess AN, Nevin A, Cheshire P, Longman GW. Macromolecules 1980;13:667.
[23] Spells SJ. In: Spells SJ, editor. Characterization of solid polymers. London: Chapman & Hall; 1994.
[24] Spells SJ. Polymer 1985;26:1921.
[25] Spells SJ, Keller A, Sadler DM. Polymer 1984;25:749.